Negligible liquid-vapor separation in the proto-lunar disk: constraints on evolution

Kaveh Pahlevan[1,2], Charles F. Gammie[3]

Abstract

Despite its importance to lunar origin, the evolution of the proto-lunar disk eludes precise description. A number of developments nevertheless make it possible to constrain this evolution. Here, we use a model of the proto-lunar disk with a silicate vapor atmosphere and a magma layer to explore the consequences of mixing across the radial extent of the disk. Four features of such a stratified disk act to radially segregate silicon isotopes by mass: (i) the magma-vapor interface exhibits a temperature gradient across the disk radial extent, (ii) silicon experiences distinct bonding environments in the magma and vapor, producing large equilibrium isotope effects between the phases, (iii) equilibration between a magma layer and a atmosphere therefore concentrates heavy isotopes into the magma, generating an isotopically light atmosphere, with the magnitude of the isotopic difference dependent on temperature. Temperature gradients are therefore translated via equilibrium partitioning into compositional gradients in the magma layer and atmosphere, (iv) radial mixing in the atmosphere results in net isotopic transport, which redistributes heavy (light) isotopes to outer (inner) disk regions. That inner disk material accretes onto Earth whereas the outer disk participates in lunar accretion permits such a redistribution process to be expressed in the composition of Earth's mantle and Moon. Existing isotopic data severely constrain the extent to which the proto-lunar disk existed in such a stratified state. The silicon isotopic constraint poses a challenge to evolutionary disk scenarios that efficiently separate proto-lunar liquids from vapors.

[1] Corresponding author kpahlevan@seti.org
[2] Carl Sagan Center, The SETI Institute, 189 Bernardo Ave, Suite 200, Mountain View, CA 94043 USA
[3] Department of Astronomy, University of Illinois at Urbana-Champaign, 1002 West Green Street, Urbana, IL 61801, USA

1. INTRODUCTION

The Moon is generally thought to have formed from a melt-vapor disk generated via the off-center impact of a planet-sized body with the proto-Earth towards the end of Earth accretion (Cameron & Ward 1976; Hartmann & Davis 1975). Such an origin via giant impact can explain the angular momentum present in the Earth-Moon (EM) system (Cameron & Ward 1976), the lunar mass and Fe deficit (Canup & Asphaug 2001), and the small but non-zero inclination of the lunar orbit (Ćuk et al. 2016; Pahlevan & Morbidelli 2015; Touma & Wisdom 1998; Ward & Canup 2000). In its simplest formulation, however, the giant impact model cannot readily explain the precise isotopic similarities between the silicate Earth and Moon (Kruijer & Kleine 2017; Pahlevan 2014) as most of the material injected into orbit is sourced from the impacting planet rather than the proto-Earth, a robust feature of all impact simulations that leave the system with its current level of angular momentum (Canup 2004; Canup & Asphaug 2001; Canup, Barr, & Crawford 2013). Here, we refer to the low-velocity, oblique, Mars-mass impact onto the proto-Earth as the "standard" impact.

Motivated by the problem of isotopic homogeneity in the EM system, three new single-impact scenarios have been proposed. First, it has been suggested that the Moon-forming impact was a hit-and-run event (Reufer et al. 2012) such that the impact could be characterized by more angular momentum than currently present in the EM system, with the excess carried off by the impacting body. Such an impact can source a somewhat higher percentage of the proto-lunar disk from Earth's mantle (~60%) than the standard scenario (~40%) and whereas this reduces the severity of the isotopic problem, it is unlikely to eliminate it entirely. Second, it has been suggested that the proto-Earth was rotating near the threshold for fission before impact — with a < 3 hour rotation period — and that a high-velocity impactor struck it nearly head-on generating a satellite-forming disk directly from proto-Earth's mantle (Ćuk & Stewart 2012). Finally, it has been proposed that the Moon-forming event may have been a nearly symmetric impact between two ~half Earth-mass bodies (Canup 2012). In this scenario, both the emerging planet and disk injected into orbit are sourced — by symmetry — equally from the impacting bodies. These last two scenarios have the potential to generate planet-satellite systems with close isotopic similarities, at least for lithophile elements (Pahlevan 2014). However, both scenarios involve an overabundance of angular momentum — by a factor of 2 or greater — relative to the modern EM system. Hence, to be reconciled with the observed dynamical state of the system, most of the angular momentum in these model systems must be transferred out. The only mechanisms that might remove this amount of angular

momentum are the evection resonance (Ćuk & Stewart 2012; Touma & Wisdom 1998), a related limit cycle (Rufu & Canup 2020; Tian, Wisdom, & Elkins-Tanton 2017; Wisdom & Tian 2015), or the Laplace plane instability (Atobe & Ida 2007; Ćuk, et al. 2016; Tian & Wisdom 2020). The efficacy of all these mechanisms depends on specific values of the tidal dissipation parameters of the post-impact Earth and Moon that are likely variable during this epoch and not well-constrained, making self-consistent thermal-orbital models difficult to construct. Magnetic winds have also been proposed as a way to carry off angular momentum but the efficacy of this mechanism for the post-impact Earth-Moon system is also unclear (Gammie, Liao, & Ricker 2016).

A different kind of solution to the problem of EM isotopic homogeneity — called equilibration — envisions a proto-lunar disk initially isotopically distinct from Earth, and invokes fluid dynamical mixing of the hot, convective, planet-disk system into a single isotopic reservoir during the ~10^3 years after the giant impact but before the cessation of lunar accretion (Lock et al. 2018; Pahlevan & Stevenson 2007). Since the Moon accretes from the outermost disk material (Salmon & Canup 2012), such a scenario requires that the proto-lunar disk undergo turbulent mixing across its radial extent. Efficient radial mixing is possible when the radial mixing timescale is short compared to the disk evolution timescale. Modeling the effect of turbulence on compositional transport via a diffusivity D and the effect of turbulence on angular momentum transport via a viscosity ν, efficient radial mixing occurs when the turbulent Schmidt number Sc($\equiv\nu/D$) is much less than unity. Sc depends on the characteristics of turbulence. Although Sc has been measured in simulations of magnetically driven disk turbulence (Carballido, Stone, & Pringle 2005), it has not yet been measured in simulations of the convectively driven turbulence that is likely present in the protolunar disk. The effective viscosity associated with convection is believed to be small (Lesur & Ogilvie 2010; Stone & Balbus 1996).

Given the suite of new ideas aimed at understanding EM isotopic homogeneity and lunar origin, we need new tools to constrain and test the various scenarios. Here, we describe development of one such tool. We show that turbulent radial mixing in a stratified proto-lunar disk — with a silicate vapor atmosphere and a separately convective midplane magma layer co-existing in equilibrium — makes specific predictions for mass-dependent isotopic offsets in the composition of lunar and terrestrial rocks. We then use the measured isotopic abundances to set constraints on how the proto-lunar disk could — and could not — have evolved.

Finally, we discuss implications for equilibration as the origin of the EM isotopic homogeneity.

2. DISK MODEL

Currently considered scenarios for a single Moon-forming giant impact (Canup 2004, 2012; Canup & Asphaug 2001; Ćuk & Stewart 2012; Reufer, et al. 2012) shock-heat and disaggregate the lunar-forming material into a hot, melt-vapor circumterrestrial disk (Nakajima & Stevenson 2014). At present, no model exists that begins with such an initial state and follows the evolution, ending with statements about the stable isotopic composition of major elements constituting the lunar-forming material. Here, we describe a numerical disk model with the goal of forging a link between disk processes and stable isotopic data on lunar and terrestrial rocks. The physical picture envisioned for protolunar disk evolution is similar to that initially envisioned for the equilibration hypothesis (Pahlevan & Stevenson 2007). The rationale for this choice is that developing the consequences of this well-defined scenario yields insights into how lunar disk evolution more generally could — and could not — have occurred.

2.1. Vertical Structure

The melt-vapor disk generated by the giant impact settles into a nearly hydrostatic state — with a vapor cloud expanding to assume a density distribution according to the local scale height — on dynamical timescales of hours to days. Radiative cooling subsequently drives the evolution of the proto-lunar disk. In the standard picture, vigorous turbulent convection is required to match high radiative losses from a ~2,000 K photosphere (Thompson & Stevenson 1988), above which the thermal structure is determined by radiative transfer. Calculation of the disk vertical structure is simplified by the fact that a negligible fraction of atmospheric mass exists above the photosphere at ~millibar pressures with the convective atmosphere extending to pressures of hundreds of bars (Thompson & Stevenson 1988). The disk atmosphere is almost entirely convective and is expected to be characterized by an adiabatic (or pseudoadiabatic) vertical structure (Holton 1992).

A major unresolved question — which has consequences for lunar composition — is whether the liquid in the proto-lunar disk exists as droplets kept in suspension via vigorous convection (Thompson & Stevenson 1988) or whether it settles into a midplane layer that dynamically decouples from the overlying atmosphere (Machida & Abe 2004; Ward 2012). We refer to these two cases as the unstratified and stratified disks, respectively. An end-member stratified disk scenario

(herein called "fully stratified") is one in which, not only is the midplane more liquid-rich than would be expected based on a single vertical disk isentrope, but the exchange of matter between the liquid layer and the atmosphere is mediated by exchange across a phase boundary, with no advective fluid motions carrying atoms directly between the two layers (e.g., no convective overshoot). In such a fully stratified scenario, elements that readily vaporize (e.g., O) will enter the atmosphere and be available to undergo radial mixing and isotopic equilibration (Pahlevan & Stevenson 2007) whereas more refractory elements (e.g., Ti) will be concentrated in the midplane liquid layer and undergo less Earth-disk equilibration. EM isotopic heterogeneity for refractory elements has been sought, but not found (Zhang et al. 2012).

Here, we assume that the disk is fully stratified: that the vertical structure consists of a convective liquid-rich midplane layer, a liquid-vapor interface, and an overlying convective atmosphere. The separately convective liquid-rich and vapor-rich columns are assumed to be in thermodynamic equilibrium at precisely defined interface conditions. Vertical mixing *within* each layer is assumed to be efficient because convective velocities are high and variations in atmospheric composition due to phase separation ("rainout") are expected to be small relative to the compositional contrast between the co-existing liquid layer and vapor atmosphere (Pahlevan, Stevenson, & Eiler 2011). Implications of relaxing the assumption of efficient vertical mixing are discussed in §4.2.

The pressure at the liquid-vapor interface is determined by hydrostatic balance with the self-gravity of the disk and the vertical component of Earth gravity:

$$-\frac{1}{\rho}\frac{\partial P}{\partial z} = 2\pi G\sigma(z) + \frac{GM_E}{r^3}z \qquad (1)$$

where ρ is the density, P is the pressure, z is the height above the midplane, G is the gravitational constant, $\sigma(z)$ is the local disk surface density enclosed at height z, M_E is the mass of Earth, and r is the radial distance in cylindrical coordinates. This equation can be integrated to yield:

$$P_{int} = \frac{\pi G \sigma_T^2}{2}\left[1-\left(1-f_v\right)^2\right] + \frac{1}{2}\Omega^2\sigma_T f_v h_{mass} \qquad (2)$$

where P_{int} is the interface pressure, σ_T is the total surface density of the column (liquid layer plus atmosphere), f_v is the mass fraction of the vapor atmosphere in the column ($\equiv\sigma_v/\sigma_T$), Ω is the Keplerian angular velocity [$\equiv(GM_E/r^3)^{1/2}$], and h_{mass} the mass-weighted scale height of the column which can be approximated as the mass-weighted height of the vapor atmosphere:

$$h_{mass} = 2\int_{z_{int}=0}^{\infty} z\rho_v(z)\,dz \Big/ \int_{-\infty}^{\infty} \rho_v(z)\,dz \qquad (3)$$

We assume that the second term in Equation (2) corresponding to the vertical component of Earth's gravity dominates, such that $h_{mass} \sim c_s/\Omega$ where c_s is the isothermal sound speed [$\equiv(kT/\mu)^{1/2}$] and μ the vapor mean molecular weight. By substituting nominal parameter values for the proto-lunar disk ($\sigma_T = 5\times10^6$ g/cm^2, $\Omega = 2\times10^{-4}$ s^{-1}, $c_s = 10^5$ cm/s) into both terms in Equation (2), the dominance of central gravity in determining disk vertical structure can be confirmed.[4] This calculation justifies neglecting disk self-gravity, as also assumed in (Ward 2012). Previous works have shown that the convective proto-lunar disk is nearly isothermal vertically due to large latent heat of condensation of silicates (Genda & Abe 2003; Thompson & Stevenson 1988). Accordingly, we adopt an isothermal vertical structure for the atmosphere with the well-known Gaussian density structure $\rho(z) = \rho(0)\exp(-z^2/H^2)$ and scale height given by $H = \sqrt{2}C_s/\Omega$. Substituting this structure into Equation (3) yields a mass-weighted height $h_{mass} = \sqrt{2/\pi}\ C_s/\Omega$, and substituting this expression into the second term in Equation (2) yields an expression for the interface pressure:

$$P_{int} = \frac{1}{\sqrt{2\pi}} f_v \sigma_T C_s \Omega \qquad (4)$$

We use this expression to relate pressure at the liquid-vapor interface to other variables describing the thermodynamic state of the disk locally.

2.2. Radial Structure

The disks injected into orbit via giant impacts are generally compact, with most of the orbiting mass confined to several planetary radii. For simplicity, we assume that the surface density profile characterizing the proto-lunar disk scales as ~1/r, as seen in simulations of the standard impact (Canup, et al. 2013). High angular momentum impacts (Canup 2012; Ćuk & Stewart 2012) tend to create even more compact disks, which may cause identifiable differences in the satellite that results (Salmon & Canup 2014). For the purpose of this work, we neglect differences in radial mass distribution. In order to make a connection between disk processes and isotopic data, we assume that the proto-lunar disk extends from 1-5 Earth radii (R_E) and that the outer disk material (from 3-5 R_E) accretes onto the Moon with its isotopic composition expressed in the lunar

[4] Equivalently, one can check that Toomre's Q parameter ($c_{gas}\Omega/\pi G\sigma$) is >> 1, implying that self-gravity is minor.

samples, whereas inner disk material (from 1-3 R_E) reaccretes back onto Earth with its compositional character diluted and essentially erased via mixing into the massive terrestrial magma ocean. In reality, the processes of disk chemical evolution studied here and of lunar accretion studied elsewhere (Salmon & Canup 2012) overlap but any coupling between these processes is beyond the scope of this work and must be subject to future modeling. Here, we restrict the study to disk processes that can cause the outer disk to acquire compositional characteristics distinct from the inner disk, a distinctness that can be expressed in the composition of Earth's mantle and Moon. Simulations find that the initial thermal structure of the impact-generated disk is radially isentropic (Nakajima & Stevenson 2014), an initial condition we adopt for calculations of the subsequent thermochemical evolution.

2.3. Thermodynamic Model

We apply a two-phase, two-component thermodynamic model expressly developed to study liquid-vapor fractionation in the aftermath of the giant impact (Pahlevan, et al. 2011) to calculate equilibrium thermodynamic conditions (e.g., T, degree of vaporization) in the proto-lunar disk. The model has been previously described; here we summarize its features and describe its current application. The silicate liquid is modeled as a binary solution of olivine end-members, $(Fe,Mg)_2SiO_4$, whereas the silicate vapor is described as a mixture of ideal gases consisting of gaseous species formed upon vaporization of such a liquid: SiO_2, SiO, Si, FeO, Fe, MgO, Mg, O_2, and O. This choice of compositional model is motivated by the fact that the bulk Moon — and therefore the proto-lunar disk — is primarily composed of ferromagnesian silicates (Taylor & Wieczorek 2014). At each time step in the evolution, we divide the proto-lunar disk into annuli and calculate equilibrium between the liquid layer and vapor atmosphere. Input parameters include the column entropy ranging from highly vaporized to condensed states (S=0.530-1.030 kJ/mol.K where mol refers to moles of olivine units or silicon atoms) and column composition (x_c=Fe/Fe+Mg), initially set equal to Earth mantle composition (≈0.1) (Jones & Palme 2000). Using equations derived from the two-phase equilibrium assumption (Pahlevan, et al. 2011), and the pressure of equilibration (Equation 4), we solve for the interface temperature (T), the column vapor fraction (f_v), the specific entropy (S_L, S_V) and composition (X_L, X_V) of the liquid and atmospheric columns, as well as the partial pressure at the interface of each of nine vapor species (P_i) at each time step and annulus.

2.4. Radial Transport

Because of the temperature-dependence of equilibrium partitioning (e.g., Equation 9), radial gradients in interface temperature in the disk are expressed as radial gradients in composition of the liquid layer and complementary atmosphere. Because the disk atmosphere features turbulent convection (Thompson & Stevenson 1988), development of compositional gradients will lead to transport of species down gradient. Hence, one consequence of an equilibrium fully-stratified (settled liquid) disk model is the development of radial atmospheric compositional gradients that — in concert with a convective atmosphere — leads to net radial transport of chemical and isotopic species. We assume that turbulent convection in the atmosphere can be characterized by an eddy diffusivity (Tennekes & Lumley 1972). In the presence of compositional gradients, atmospheric motions will then transport species in accordance with Fick's law:

$$\boldsymbol{J}_i = -\rho_v D_v \nabla \boldsymbol{c}_{i,v} \quad (5)$$

where J_i [kg m^{-2} s^{-1}] is the mass flux of an atmospheric constituent i, ρ_v is atmospheric mass density, D_v is turbulent diffusivity, and $c_{i,v}$ is mass fraction of constituent i. In principle, a similar equation could be written for turbulent mixing in the magma layer. However, because of both greater length scales and velocity scales associated with atmospheric convection, radial transport is dominated by atmospheric motions (Pahlevan & Stevenson 2007). Accordingly, we consider a liquid layer that is stationary but rapidly equilibrating with the turbulent atmosphere. We take the divergence of Equation (5), and combine it with a continuity equation:

$$\frac{\partial\left(\rho_v c_{i,v}\right)}{\partial t} = -\nabla \cdot \left(\rho_v D_v \nabla \boldsymbol{c}_{i,v}\right) \quad (6)$$

to describe atmospheric transport. Using the continuity equation here without sources or sinks is valid for species that are neither created nor destroyed. Atomic abundances can be described in this way but molecular abundances cannot due to the occurrence of chemical reactions. Such an equation is only used to describe compositional changes in the atmosphere and compositional changes to the liquid layer arising from liquid-vapor equilibration are treated separately in the model. The reason for this separate treatment is that — unlike signatures that are identical between a silicate liquid and co-existing vapor (e.g., $\Delta^{17}O$ studied in (Pahlevan & Stevenson 2007)) — here we are considering chemical and isotopic signatures that are distinct between co-existing phases (e.g., $^{30}Si/^{28}Si$, see §2.6). Expecting rapid vertical mixing but rate-limiting radial mixing in the disk, we integrate Equation (6) vertically through the atmosphere:

$$\sigma_v \frac{\partial c_{i,v}}{\partial t} = -\nabla \cdot \left(\sigma_v D_v \nabla c_{i,v} \right) \quad (7)$$

where $\sigma_v (\equiv f_v \sigma_T)$ is the atmospheric surface density [kg m^{-2}]. We assume that this parameter has no time-dependence arising from disk turbulence, because turbulent convection leads to little net mass transfer. Indeed, numerical studies of disks have found that convection does not efficiently transport angular momentum (Lesur & Ogilvie 2010; Stone & Balbus 1996), a requirement for net mass transport. This issue is further discussed in §4.1. Atmospheric surface density does vary in the model due to thermal evolution (i.e., condensation, §2.5). At each time step, we use Equation (7) in cylindrical coordinates to describe changes in atmospheric composition with zero net flux boundary conditions, $\partial c / \partial r\left(R_E, t \right) = \partial c / \partial r\left(5R_E, t \right) = 0$, reflecting the simplification of neglecting moonlet formation and satellite-disk interactions in the outer disk (Salmon & Canup 2012) and neglecting turbulent mixing with the silicate vapor atmosphere of Earth in the inner disk (Lock, et al. 2018; Pahlevan & Stevenson 2007). Different boundary conditions are possible, but here we make this choice in order to study processes within the proto-lunar disk itself, relegating interactions with its environment to future works.

2.5. Thermal Evolution

The viscous and thermal evolution of the proto-lunar disk is a closely coupled problem. The material in the proto-lunar disk is susceptible to gravitational instability (Cameron & Ward 1976) with a viscous evolution timescale for particles of order ~1 year (Ward & Cameron 1978). Such a rapid evolutionary timescale liberates enough gravitational energy for the material to self-vaporize, violating the original particle assumption (Thompson & Stevenson 1988). Hence, the proto-lunar disk is thought to be thermally regulated, whereby heating due to viscous gravitational energy release would be controlled by radiative losses. Accordingly, subsequent works explore coupled solutions to the viscous and thermal evolution (Charnoz & Michaut 2015; Gammie, et al. 2016; Ward 2012). Here, we adopt a simplified thermal history in which radiative losses are powered by secular cooling alone; we do not consider viscous heating. The motivation for, and limitations of, this assumption are discussed in §4.1.

Treating radiative cooling as a quasistatic process, we relate the outgoing heat and entropy fluxes using the thermodynamic identity, $dQ = TdS$, where T is the temperature of the radiated photons. Further approximating the radiation as

a blackbody, we write an expression for the entropy per unit area being radiated from both sides of the proto-lunar disk per unit time:

$$dS = 2\sigma_{SB} T_{ph}^{3} dt \quad (8)$$

where σ_{SB} is the Stefan-Boltzmann constant, T_{ph} is the photospheric temperature. We can use this expression to calculate radiative entropy losses from disk annuli. Because of vertical convection, the effects of radiative cooling rapidly propagate down through the column; equivalently, the entire thermal reservoir of the disk is tapped by radiative losses. At each time step, new values of entropy are derived for each annulus after radiative losses, whereas radial transport (§2.4) and liquid/vapor re-equilibration (§2.3) are calculated using an operator split scheme, i.e., calculating the effects of each process in sequence.

We follow the thermal evolution of the disk from an initial to a final state. Motivated by the impact simulations, we adopt initial thermal states — expressed as vapor fraction — ranging from mostly (~80%) liquid (Canup 2004) to mostly (50-95%) vapor (Canup 2012; Ćuk & Stewart 2012). For final states, because we are interested in articulating expected compositions of the outer disk material, and because atmospheric transport dominates convective transport in the liquid layer (§2.4), when the vapor in the outer disk (3-5 R_E) has fully condensed (f_v < 0.01), the composition of the liquid is considered frozen-in, to be later expressed in the isotopic composition of the Moon and its rock samples. Hence, we consider the evolution until condensation of the outer disk. In addition to neglecting viscous heating, we do not consider turbulent radial transport of entropy and heat in the atmosphere, or other possible triggers of compositional freeze-in, e.g., disk fragmentation into moonlets, but discuss possible variations in disk models in §4.2 and §4.3.

2.6. Silicon Isotopes as Tracers

We choose silicon isotopes as tracers for several reasons. First, at high temperature, equilibrium isotopic differences between co-existing phases approach zero (Urey 1947) and small but significant isotopic fractionation is only possible where there are significant differences in bonding environment between the phases present for the element under consideration. Silicon, for example, exists as SiO_4^{-4} in silicate melts and predominantly as SiO in co-existing vapors (Visscher & Fegley 2013), permitting large liquid-vapor isotopic fractionation (~0.5 per mil in $^{30}Si/^{28}Si$) in the high-temperature environment (~3,000-4,000 K) encountered during lunar origin (Pahlevan, et al. 2011).

Second, unlike magnesium, iron, and oxygen, which significantly reside in multiple gas species in silicate vapors, SiO dominates the vapor speciation of silicon (e.g., over SiO_2 and Si) for the full range of conditions in the proto-lunar disk (Visscher & Fegley 2013). Because of such a simple monopoly in vapor speciation, even a two-component thermodynamic model (§2.3) accurately captures the speciation of silicon in the proto-lunar disk, a requirement for accurately articulating predictions of isotopic fractionation in evolutionary scenarios. Finally, to forge a connection with the observable data, we require an element whose isotopic abundances in Earth's mantle and Moon are precisely known. Because the bonding environment for silicon in silicate melts and crystals are similar (Huang et al. 2014), substantial silicon isotopic variations are not generated during ordinary (i.e., crystal-liquid) petrologic processes such as mantle melting (Zambardi et al. 2013) or during magma ocean crystallization. Hence, the isotopic composition of Earth's mantle and Moon can be derived from measurements on samples and are known to high precision, permitting comparison of the observational data with predictions of post giant-impact liquid-vapor evolution (Armytage et al. 2012; Pahlevan 2014) without any substantial signal degradation from subsequent geological processes, to which silicon isotopes are essentially impervious.

Silicon isotopes are considered as passive tracers. At each time step, liquid-vapor equilibrium at each annulus is characterized by a temperature, T (§2.3). Because the isotopic fractionation is only a function of temperature in this low-pressure (<1GPa) system, we calculate the partitioning of Si isotopes between the silicate liquid and vapor as:

$$\Delta_{L-V} = 5\left(10^3/T\right)^2 \; per\ mil \qquad (9)$$

$$\delta_C = F_V^{Si}\delta_V + \left(1 - F_V^{Si}\right)\delta_L \qquad (10)$$

where $\Delta_{L\text{-}V}=\delta_L-\delta_V$ is the part per thousand difference of the $^{30}Si/^{28}Si$ between the liquid and vapor, as previously calculated using standard procedures (Pahlevan, et al. 2011) and δ_L, δ_V, δ_C represent the isotopic compositions of the liquid layer, the vapor atmosphere, and the entire column. We set the initial disk composition $\delta_C(r,0)$ to zero for reference. In this way, we calculate radial isotopic structure of the proto-lunar disk atmosphere and liquid layer, given a radial disk compositional [$\delta_c(r,t)$] and thermal [T(r,t)] structure. Two features of the isotopic partitioning are notable. First, $\Delta_{L\text{-}V}$ is positive, such that the heavier isotopes of silicon concentrate into silicate liquids. Second, the temperature dependence of the fractionation guarantees spatial variations in the liquid-vapor partitioning in the proto-lunar disk. In particular, the

radial gradient in equilibration temperature will be expressed — through equilibrium partitioning (Equation 9) — as silicon isotopic gradients in the atmosphere and liquid layer. Once this equilibrium state is calculated, we propagate the evolution forward by calculating the radial isotopic transport via Equation (7), where $c_{i,v}$ now represents δ_v. After calculating radial transport, we permit the atmosphere — now out of equilibrium with the liquid layer — to re-equilibrate, thereby changing the composition of the lunar-forming liquid. In this way, turbulent motions in the convective vapor atmosphere can change the isotopic composition of a quasi-stationary Moon-forming liquid. In the case of silicon, such isotopic redistribution tends to concentrate the heavy isotopes in the outer (i.e., Moon-forming) regions of the disk.

3. RESULTS

3.1. Thermal State and History

Because of the weak (logarithmic) dependence of the entropy of ideal gases on pressure, the initial isentropic state of the proto-lunar disk translates to a radially ~constant vapor fraction initially (Figure 1a). Because of high latent heat of condensation and high vapor fractions (~tens of percent), the secular cooling heat budget of the proto-lunar disk is dominated by latent heat of condensation, with minor contributions from sensible heat ($c_p\Delta T$). Hence, unlike the post-impact atmosphere of Earth which is thermally buffered from below, secular cooling of the proto-lunar disk in the absence of viscous heating is rapid. Because of an outwardly decreasing surface density profile, the disk first cools at large distances with a condensation front that propagates inwards on a timescale of years (Figure 1a).

The temperature structure of the disk has several notable features. First, even at the outset of the evolution, an isentropic disk is characterized by a significant radial temperature gradient, as also observed in (Nakajima & Stevenson 2014). Second, because of more rapid cooling in the outer disk, the radial T-gradient of the disk steepens with time, ranging from 125-350 K/R_E (Figure 1b). The existence of such a radial temperature gradient is expected to be a universal feature of any proto-lunar disk model and plays a central role in the evolution of isotopic signatures considered below.

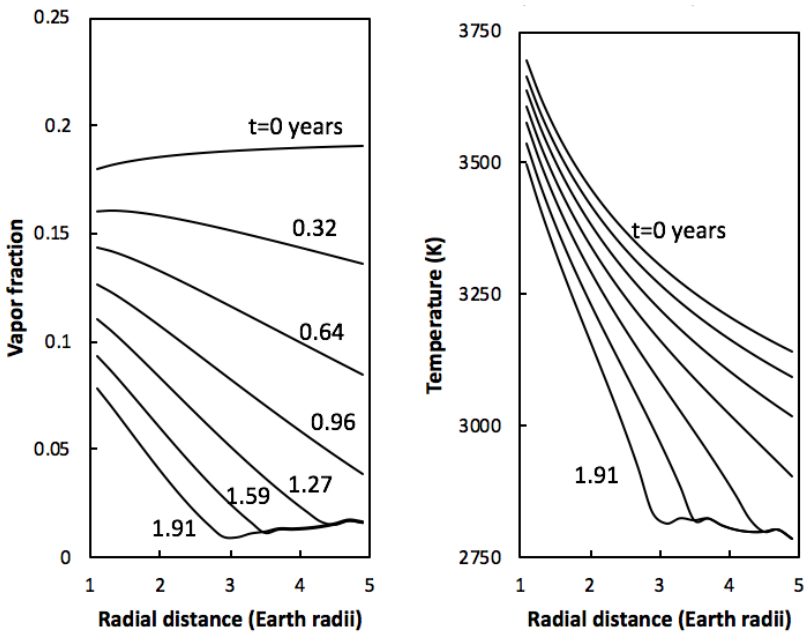

Figure 1. Disk thermal state and evolution. (a) Disk vapor fraction (atmospheric mass / total disk column mass) versus radial distance. This cooling history corresponds to an initial condition (f_v~0.2) generated via the "standard" impact. The simulations are halted at f_v~0.01 for numerical reasons. (b) Equilibration temperatures at the liquid-vapor interface versus radial distance. Note that, even in an initially isentropic disk, the disk is characterized by a radial temperature gradient due to the radial pressure gradient arising from, e.g., radial surface density gradients in the disk, and cooling of the disk only accentuates a pre-existing T-gradient.

3.2. Major Element Chemical Fractionation

The two-component [$(Fe,Mg)_2SiO_4$] thermodynamic model adopted has one variable for chemical composition, x_{Fe}(≡Fe/Fe+Mg), making possible studies of chemical fractionation. Accordingly, we track the x_{Fe} of the liquid, vapor, and total column in the proto-lunar disk during the evolution. As has been experimentally determined, fayalite (Fe_2SiO_4) has a higher vapor pressure than forsterite (Mg_2SiO_4) at identical temperature (Nagahara, Kushiro, & Mysen 1994), a behavior clearly expressed in the proto-lunar disk: the vapor atmosphere is enriched in FeO (x_{Fe}=0.12-0.35), while the liquid layer is FeO-depleted (x_{Fe}=0.02-0.06), relative to the composition of the column as a whole (x_{Fe}=0.1, Figure 2a). Moreover, due to the temperature and pressure gradients in the disk, even an

initial chemical homogeneity will – through equilibrium partitioning – result in radial chemical gradients in liquid and atmospheric reservoirs. An increasing iron oxide content of the vapor atmosphere with radius (Figure 2a) implies an inward turbulent transport of iron in the atmosphere arising from convective mixing. Through liquid-vapor re-equilibration, atmospheric transport of species also leads to the development of chemical gradients in the lunar-forming liquid. In this way, turbulent transport can be expected to redistribute chemical species in the proto-lunar disk.

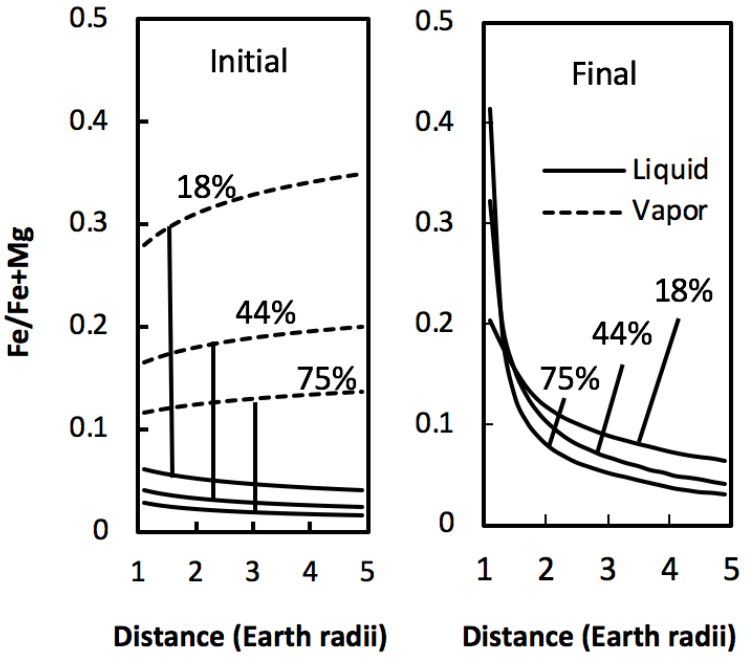

Figure 2. Fe/Mg redistribution in the proto-lunar disk. (a) Initial liquid-vapor partitioning in a disk with bulk x_{Fe}(Fe/Fe+Mg)=0.1. The percentage labels on curves correspond to initial disk vapor fraction. (b) Final compositional structure of the disk when the vapor has condensed and the liquid composition has frozen in. The vigor of turbulence in these simulations is $\alpha=3\times10^{-3}$.

Two features of turbulent chemical transport are notable: (i) the outer disk material from which the Moon forms is modestly depleted in iron-rich silicates relative to the inner disk, which falls back onto Earth (Figure 2b). The sign of this fractionation can be understood as follows: as the outermost disk condenses, it becomes increasingly iron-rich (Figure 2a), such that turbulent

mixing with the hotter, more highly vaporized inner disk depletes FeO from the lunar-forming material, (ii) the magnitude of chemical fractionation is modestly dependent on initial disk vapor fraction (Figure 2b). This result can be understood because higher vapor fractions are associated with longer secular cooling timescales (§3.1), permitting the chemical redistribution to proceed longer, and because it implies a greater atmospheric mass relative to the mass of the quasi-stationary melt layer, permitting more efficient turbulent transport and steeper chemical gradients to develop per unit time. For the major elements here considered, the redistribution is small but non-negligible: for the range of initial vapor fractions considered for the proto-lunar disk, the resulting depletion in outer disk Fe/Fe+Mg is < 2x. Hence, impact models that begin with an Earth-mantle-like disk (Canup 2012; Ćuk & Stewart 2012) cannot generate an FeO-enriched silicate Moon (Jones & Palme 2000) via turbulent redistribution: some other process is required (Pahlevan, et al. 2011). Nevertheless, due to uncertainties in both the initial Fe/Fe+Mg in the proto-lunar disk as well as in the lunar bulk chemical composition, modest chemical fractionation in the proto-lunar disk is difficult to rule out using major elements. We conclude that the major element composition of the Moon places only modest constraints on chemical fractionation processes in the proto-lunar disk.

3.3. Silicon Isotope Fractionation

Equilibrium silicon isotopic fractionation is significant, resulting in a ~0.4-0.5 per mil offset between the $^{30}Si/^{28}Si$ of silicate liquids and vapors at the temperatures prevailing in the proto-lunar disk (Figure 3a). As discussed in §2.6, the proto-lunar liquid concentrates the heavy isotopes of silicon whereas the complementary vapor atmosphere is isotopically light, with the difference between the two reservoirs increasing with increasing radius, due to the negative radial temperature gradient (Figure 1b) and equilibrium partitioning law (Equation 9), which dictates enhanced fractionation at lower temperatures. The resulting composition of the atmosphere exhibits greater isotopic lightness with increasing radial distance and implies an inward transport of light silicon isotopes accompanying turbulent convection in the atmosphere. Liquid-vapor equilibration transmits this signal to the proto-lunar liquid and the process continues until the proto-lunar disk has condensed and the isotopic structure has frozen in. As with chemical fractionation (§3.2), steeper gradients are generated from hotter initial states (Figure 3b), the reasons being two-fold: longer cooling timescales and greater atmospheric masses causing greater

transport and redistribution during the cooling history as a by-product of turbulent convection.

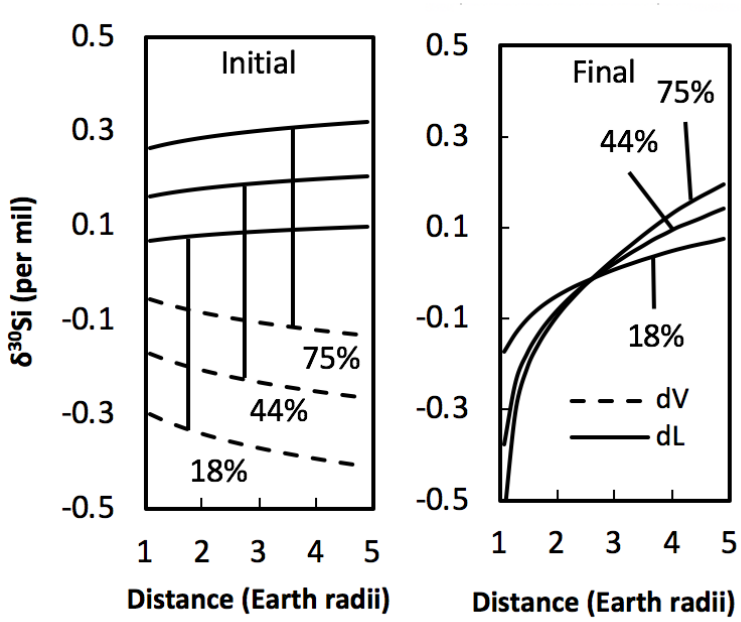

Figure 3. Silicon isotopic fractionation in the proto-lunar disk. (a) The initial radial isotopic structure of the proto-lunar disk atmosphere and liquid layer, with disks assumed to have a radially uniform initial composition set to zero for reference (δ^{30}Si=0). The number labels on the curves correspond to the initial disk vapor fraction. Equilibrium partitioning leads to a liquid layer that is isotopically heavy with a complementary isotopically light vapor atmosphere. (b) Final isotopic structure of the disk at the end of the thermal history when the vapor has condensed and the liquid composition has frozen in. The increasing isotopic lightness of the vapor atmosphere with radius implies in an inward transport of light isotopes whose magnitude depends on the disk initial vapor fraction.

The magnitude of the silicon isotope fractionation is large relative to the precision with which the composition of terrestrial and lunar reservoirs is measured, permitting the development of a new stable isotopic constraint on the evolution of the proto-lunar disk. As is also true for chemical fractionation (§3.2), both more vigorous turbulence (higher α) and hotter initial thermal states result in greater isotopic fractionation between the outer (i.e., Moon-forming) and inner proto-lunar disk (Figure 4). For nominal values of turbulent

diffusivity (α=3x10^{-3}), even modestly vaporized proto-lunar disks (f_v~0.2-0.4) can imprint measurable mass-dependent signatures onto the lunar forming material ($\delta^{30}Si_M$=0.05-0.1‰ — Figure 4). An Earth-Moon isotopic offset of this magnitude can be excluded with existing data (Armytage, et al. 2012; Fitoussi & Bourdon 2012). Possible interpretations of the data in light of the model results are discussed in §4.4.

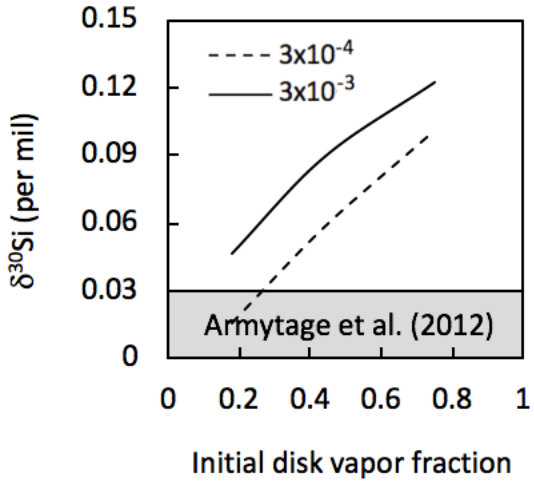

Figure 4. Summary of silicon isotopic redistribution in the proto-lunar disk. The average isotopic composition of the outer Moon-forming disk (3-5R_E) is plotted as a function of the initial vapor fraction for two different values of the turbulent α parameter. The initial composition of the disk (δ^{30}Si) is set to zero in these calculations for reference. In the absence of radial diffusivity, the final and initial composition of the outer disk would be identical, but for even modest levels of turbulence (α=3x10^{-4}-3x10^{-3}), measurable isotopic differences between the inner and outer disk can evolve. Measurements on terrestrial and lunar samples observe no δ^{30}Si difference between the Earth and Moon (Δ^{30}Si-EM=$\delta^{30}Si_E$-$\delta^{30}Si_M$) at a precision of < 0.03 per mil (Armytage, et al. 2012; Fitoussi & Bourdon 2012). Possible interpretations are discussed in §4.

4. DISCUSSION

We have described a coupled thermochemical model for the evolution of the proto-lunar disk with the goal of forging a link between the stable isotopic composition of the lunar-forming material and the parameters governing lunar

525 disk evolution. Here, we discuss several simplifying features of the adopted
526 disk model, compare with other disk models discussed in the literature (§4.1-
527 4.3), and then consider the general conclusions that can be drawn about the
528 evolution of the proto-lunar disk using the constraints provided by the stable
529 isotopic data (§4.4).
530
531 4.1. Viscous Evolution
532 The model we have described neglects the viscous redistribution of mass and
533 angular momentum and the attendant gravitational energy release. Including
534 viscous evolution into the disk model would have several effects: (1) thermal:
535 due to the depth of the terrestrial gravity well, viscous spreading has
536 significant thermal consequences; where viscous heating takes place, it can
537 easily dominate the heat budget of the melt-vapor column. For example, (Ward
538 2012) described a disk model characterized by a stratified melt-vapor structure
539 with a viscous melt layer and an inviscid atmosphere, and derived a cooling
540 timescale for the proto-lunar disk of ~250 years, to be compared with a cooling
541 timescale of ~2 years for a f_v~0.2 disk powered by secular cooling alone (§3.1).
542 Hence, one consequence for the purely secular cooling powered disk model here
543 described is that the lifetime — and the magnitude of chemical and isotopic
544 redistribution calculated for the proto-lunar disk — are lower limits. The
545 lifetime and degree of chemical fractionation is expected to be greater —
546 perhaps much greater — in a model such as that described in (Ward 2012), (2)
547 transport/redistribution: viscous dissipation causes net outward transport of
548 angular momentum and net inward transport of mass and causes material to spread
549 radially, a flow that competes with turbulent mixing (Stevenson 1990). Hence,
550 by neglecting the viscous evolution, we implicitly only consider diffusive ($D/\nu \geq 1$)
551 transport regimes. We have focused on this regime because it is in this
552 regime in which extensive turbulent mixing can take place (Pahlevan & Stevenson
553 2007). However, even if a partially vaporized disk is initially in the diffusive
554 regime, it is possible that — as the disk condenses — it transitions to the
555 viscous regime ($D/\nu \leq 1$) and radial mixing becomes inefficient. The calculations
556 here presented only apply to redistribution in the diffusive regime.
557
558 4.2. Heat and Entropy Transport
559 We have considered turbulent transport in the presence of compositional
560 gradients, but neglected the equivalent transport of heat in the presence of
561 entropy gradients. It is known that — in the presence of radial entropy gradients
562 — a disk instability may arise at the expense of the entropy gradient ("radial
563 convection") and thereby radially transport heat and entropy (Klahr &

Bodenheimer 2003; Lesur & Papaloizou 2010). In the proto-lunar disk, such a radial entropy gradient may arise via preferential cooling or vertical phase separation of droplets ("rainout") in adjacent annuli of the proto-lunar disk. This process would have consequences for the calculations here presented: (1) thermal: since heat transport is outward, to the extent that this process takes place, it prolongs the thermal history and accentuates the chemical/isotopic signals that arise, and (2) compositional: since the effective gravity in the near-Keplerian disk is inwards, this process would also buoyantly exchange vapor-rich (isotopically light) atmospheric parcels with more droplet-laden (isotopically heavy) parcels radially and may therefore moderate the magnitude of radial transport here calculated and soften the constraint here described. However, we see no reason to suppose that this effect would precisely cancel the isotopic fractionation based on the radial temperature gradient calculated in this work. In the absence of such a reason, the possibility of a fortuitous cancellation of two competing effects is considered unlikely. The constraints on disk evolution are therefore considered robust to inclusion of this process.

4.3. Criterion for Compositional Freeze-in

Whereas adopting initial conditions for disk evolution from the output of giant impact simulations is straightforward, selecting a criterion for the cessation of disk evolution is less certain. Here, we have considered a disk with chemical and isotopic redistribution but no net mass transport and no fragmentation. In such a model, the condensation of the vapor atmosphere can be expected to halt radial redistribution because the turbulent atmosphere is the agent that causes transport. However, other criteria for compositional freezing of the disk are possible. (Canup et al. 2015) considered a settled disk with a viscous liquid-rich midplane layer. In analogy with particle disks, the midplane liquid layer was assumed to undergo gravitational instability and fragmentation to form moonlets beyond the classical Roche radius at 2.9 R_E defined by lunar-density condensates. (Thompson & Stevenson 1988) instead considered a disk model in which a single vertical isentrope characterized convective columns from the midplane up to the rarified regions where the disk atmosphere is optically thin and radiative. In such a picture, radiative cooling in disk patches is balanced by gravitational energy release until the material spreads to radii where this equality can no longer be satisfied, at which point the patch instabilities lead to collapse and moonlet formation and the composition of the moonlets is the composition of the disk fragment with its constituent droplets and vapor. Regardless of the precise criterion for compositional freeze-in for disk patches, it is clear that the liquid composition is effectively frozen-in once

603 the atmosphere condenses. Moreover, satellite-disk interaction may be important
604 (Salmon & Canup 2012) but its coupling to disk evolution is relegated to future
605 works.
606
607 4.4. Consequences for Disk Evolution
608 We do not know — a priori — how the proto-lunar disk evolved. Here, we have
609 considered a disk model in which the liquid settles out into a midplane layer
610 that rapidly equilibrates with the overlying atmosphere, with the turbulent
611 diffusivity in the vapor atmosphere operating on a shorter timescale than
612 viscous dissipation in either the atmosphere (Carballido, Desch, & Taylor 2016)
613 or the melt-rich layer (Ward 2012). This is the same settling and transport
614 regime originally envisaged in the equilibration hypothesis (Pahlevan &
615 Stevenson 2007) and therefore provides constraints on any evolutionary scenario
616 of this kind. We have shown that in such a picture the proto-lunar disk is
617 expected to generate isotopic gradients that would be expressed as differences
618 in the composition of the Earth's mantle and Moon. Such an Earth-Moon isotopic
619 offset is not observed to a precision of 30 ppm in the case of silicon ($^{30}Si/^{28}Si$)
620 (Armytage, et al. 2012; Fitoussi & Bourdon 2012). In light of the isotopic data,
621 the model results can be interpreted in four ways: (1) imperfect settling: the
622 proto-lunar liquid may fail to settle into a liquid-rich layer with a separately
623 convective atmosphere and instead, exchange between the midplane and vapor
624 atmosphere may be advective (e.g., convective overshoot), as also described in
625 (Thompson & Stevenson 1988). In such a scenario, equilibration and mixing with
626 the Earth would involve both a vapor atmosphere as well as the suspended liquid
627 droplets, and one would expect isotopic homogeneity in the Earth-Moon system
628 for all elements irrespective of volatility (Zhang, et al. 2012), (2) liquid-
629 vapor equilibration: we have assumed that liquid-vapor equilibrium in the system
630 is rapid relative to transport timescales. Although the vigor of convective
631 motion makes this possible, the timescale for liquid-vapor equilibration may
632 depend on foam-physics at the liquid-vapor interface and is therefore difficult
633 to quantify. Hence, one interpretation of the silicon isotopic data is that the
634 proto-lunar disk liquid and vapor underwent phase separation into two distinct
635 layers but did not experience continuous and rapid chemical re-equilibration.
636 Although large depletions of volatile elements in the lunar material suggest
637 that nearly all proto-lunar liquid equilibrated with some vapor, a timescale
638 for liquid-vapor equilibration comparable to evolutionary timescales cannot be
639 ruled out, (3) other transport regimes: we have restricted the discussion here
640 to transport regimes in which the total diffusivity is greater than the total
641 viscosity ("the diffusive regime") such that mixing can outcompete disk

spreading and homogenize the vapor atmosphere on a rapid timescale. This regime may be appropriate for a disk whose dominant instability is the convective instability, because convection in disks is known to produce turbulent mixing but weak angular momentum transport (Lesur & Ogilvie 2010; Stone & Balbus 1996). However, there exist other instabilities, e.g., the gravitational instability, that may entail different mixing and transport properties. Hence, it is also possible that the disk spent part of its evolution in the viscous regime not subject to the diffusive redistribution process here calculated, (4) high-temperature silicate thermodynamics: it is possible that a binary olivine thermodynamics does not accurately capture the vaporization behavior of silicon for the full range of thermal states experienced by the proto-lunar disk. In particular, olivine is known to vaporize congruently (Nagahara, et al. 1994) such that the degree of bulk vaporization and the degree of silicon vaporization are equivalent in an olivine thermodynamics. A more complex multi-component model may not display this behavior, instead revealing silicon isotopes to be highly sensitive to the evolution of the proto-lunar disk for only a range of vapor fractions. The degree to which olivine thermodynamics accurately captures the vaporization behavior of any given element in the proto-lunar disk can be determined by development of more complex models of multi-component silicate melts at the temperatures (T=3,000-4,000 K) of relevance.

5. CONCLUSIONS

Recent isotopic observations on lunar and terrestrial rocks indicate that the lunar material is derived from the silicate Earth. The disk stage of lunar origin has been invoked to explain several observed features of the Earth-Moon system, including the precise isotopic homogeneity (Lock, et al. 2018; Pahlevan & Stevenson 2007) and the lunar volatile depletion (Canup, et al. 2015; Nie & Dauphas 2019). Nevertheless, a quantitatively constrained description of proto-lunar disk evolution is lacking. Despite uncertainty in the initial thermal state, the settling and transport regimes, and the degree of thermal and chemical coupling to the post-impact Earth, it is well established that the proto-lunar disk experiences a two-phase (liquid-vapor) evolution. Here, we have developed a thermochemical scenario of disk evolution incorporating silicon isotopes as passive tracers. Our results demonstrate that silicon isotopic fractionation in the proto-lunar disk is significant relative to the precision of existing measurements, yielding a new constraint on disk evolution. The principal conclusion of the model is that a “settled” proto-lunar disk in the diffusive regime would have developed isotopic offsets in the silicate EM system that are not observed. Hence, it is possible to use silicon isotopes to set

constraints on Earth-disk equilibration: if system-wide turbulent mixing of the Earth-Moon system took place, it must have involved advective mixing of the proto-lunar liquid and the vapor atmosphere (e.g., with suspended droplets). More generally, the silicon isotopic identity of Earth's mantle and Moon poses a challenge to any model of the proto-lunar disk in which the liquid and vapor experience divergent fates, with one phase being preferentially reaccreted to the Earth (Canup, et al. 2015; Charnoz & Michaut 2015; Lock, et al. 2018; Nie & Dauphas 2019; Wang et al. 2019). Whether these evolutionary scenarios can be reconciled with the silicon isotopic homogeneity of the EM system remains to be investigated. These results open a new quantitative window into the evolutionary aftermath of the lunar-forming giant impact.

ACKNOWLEDGEMENTS

This work was supported in part by the Poincaré Fellowship. K.P. acknowledges discussions with David Stevenson, Robin Canup, and Sebastien Charnoz. We would like to dedicate this paper to the memory of Bill Ward, who pioneered the study of the proto-lunar disk.

REFERENCES

Armytage, R. M. G., Georg, R. B., Williams, H. M., & Halliday, A. N. 2012, Geochimica Et Cosmochimica Acta, 77, 504
Atobe, K., & Ida, S. 2007, Icarus, 188, 1
Cameron, A. G. W., & Ward, W. R. 1976, Lunar Sci, 7, 120
Canup, R. M. 2004, Icarus, 168, 433
---. 2012, Science, 338, 1052
Canup, R. M., & Asphaug, E. 2001, Nature, 412, 708
Canup, R. M., Barr, A. C., & Crawford, D. A. 2013, Icarus, 222, 200
Canup, R. M., Visscher, C., Salmon, J., & Fegley Jr, B. 2015, Nature Geosci, 8, 918
Carballido, A., Desch, S. J., & Taylor, G. J. 2016, Icarus, 268, 89
Carballido, A., Stone, J. M., & Pringle, J. E. 2005, Monthly Notices of the Royal Astronomical Society, 358, 1055
Charnoz, S., & Michaut, C. 2015, Icarus, 260, 440
Ćuk, M., Hamilton, D. P., Lock, S. J., & Stewart, S. T. 2016, Nature, 539, 402
Ćuk, M., & Stewart, S. T. 2012, Science, 338, 1047
Fitoussi, C., & Bourdon, B. 2012, Science, 335, 1477
Gammie, C. F., Liao, W.-T., & Ricker, P. M. 2016, The Astrophysical Journal, 828, 58
Genda, H., & Abe, Y. 2003, Earth Planets and Space, 55, 53
Hartmann, W. K., & Davis, D. R. 1975, Icarus, 24, 504
Holton, J. R. 1992, An Introduction to Dynamic Meteorology (San Diego: Academic Press)
Huang, F., Wu, Z., Huang, S., & Wu, F. 2014, Geochimica et Cosmochimica Acta, 140, 509

Jones, J. H., & Palme, H. 2000, in Origin of the Earth and Moon, eds. K. Righter, & R. M. Canup (Tucson, AZ: University of Arizona Press), 197
Klahr, H. H., & Bodenheimer, P. 2003, The Astrophysical Journal, 582, 869
Kruijer, T. S., & Kleine, T. 2017, Earth and Planetary Science Letters, 475, 15
Lesur, G., & Ogilvie, G. I. 2010, Monthly Notices of the Royal Astronomical Society: Letters, 404, L64
Lesur, G., & Papaloizou, J. C. 2010, Astronomy & Astrophysics, 513, A60
Lock, S. J., Stewart, S. T., Petaev, M. I., Leinhardt, Z., Mace, M. T., Jacobsen, S. B., & Cuk, M. 2018, Journal of Geophysical Research: Planets, 123, 910
Machida, R., & Abe, Y. 2004, Astrophysical Journal, 617, 633
Nagahara, H., Kushiro, I., & Mysen, B. O. 1994, Geochimica Et Cosmochimica Acta, 58, 1951
Nakajima, M., & Stevenson, D. J. 2014, Icarus, 233, 259
Nie, N. X., & Dauphas, N. 2019, The Astrophysical Journal Letters, 884, L48
Pahlevan, K. 2014, Philosophical Transactions of the Royal Society a-Mathematical Physical and Engineering Sciences, 372
Pahlevan, K., & Morbidelli, A. 2015, Nature, 527, 492
Pahlevan, K., & Stevenson, D. J. 2007, Earth and Planetary Science Letters, 262, 438
Pahlevan, K., Stevenson, D. J., & Eiler, J. M. 2011, Earth and Planetary Science Letters, 301, 433
Reufer, A., Meier, M. M. M., Benz, W., & Wieler, R. 2012, Icarus, 221, 296
Rufu, R., & Canup, R. M. 2020, Journal of Geophysical Research: Planets, 125, e2019JE006312
Salmon, J., & Canup, R. M. 2012, Astrophysical Journal, 760
---. 2014, Philosophical Transactions of the Royal Society a-Mathematical Physical and Engineering Sciences, 372
Stevenson, D. J. 1990, Astrophysical Journal, 348, 730
Stone, J. M., & Balbus, S. A. 1996, Astrophysical Journal, 464, 364
Taylor, G. J., & Wieczorek, M. 2014, Philosophical Transactions of the Royal Society a-Mathematical Physical and Engineering Sciences, 372
Tennekes, H., & Lumley, J. L. 1972, A First Course on Turbulence (Cambridge, Massachusetts: The MIT Press)
Thompson, C., & Stevenson, D. J. 1988, Astrophysical Journal, 333, 452
Tian, Z., & Wisdom, J. 2020, Proceedings of the National Academy of Sciences, 117, 15460
Tian, Z., Wisdom, J., & Elkins-Tanton, L. 2017, Icarus, 281, 90
Touma, J., & Wisdom, J. 1998, Astronomical Journal, 115, 1653
Urey, H. C. 1947, Journal of the Chemical Society, 562
Visscher, C., & Fegley, B. 2013, Astrophysical Journal Letters, 767
Wang, X., Fitoussi, C., Bourdon, B., Fegley, B., & Charnoz, S. 2019, Nature Geoscience, 12, 707
Ward, W. R. 2012, Astrophysical Journal, 744
Ward, W. R., & Cameron, A. G. W. 1978, in Lunar and Planetary Science Conference IX (Houston, Texas)
Ward, W. R., & Canup, R. M. 2000, Nature, 403, 741
Wisdom, J., & Tian, Z. L. 2015, Icarus, 256, 138
Zambardi, T., Poitrasson, F., Corgne, A., Meheut, M., Quitte, G., & Anand, M. 2013, Geochimica Et Cosmochimica Acta, 121, 67
Zhang, J. J., Dauphas, N., Davis, A. M., Leya, I., & Fedkin, A. 2012, Nature Geoscience, 5, 251

765